IEICE TRANS. COMMUN., VOL.E84–B, NO.7 JULY 2001

LETTER

Results of Link-Level Simulations Using Field Measurement Data for an FTDL-Spatial/ MLSE-Temporal Equalizer

Takefumi YAMADA[†], **Shigeru TOMISATO**[†], **Tadashi MATSUMOTO**[†], ***Regular Members***, ***and*** **Uwe TRAUTWEIN**[††], ***Nonmember***

SUMMARY This letter shows the results of a series of link level simulations conducted to evaluate the performances of spatial and temporal equalizers (S/T-equalizers) using field measurement data. The configuration of the spatial and temporal equalizer discussed in this letter can be expressed as a cascade of an adaptive array antenna and maximum likelihood sequence estimator (MLSE): each of the adaptive array antenna elements has a fractionally spaced tapped delay line (FTDL), and the MLSE has taps covering a portion of channel delay profile. Bit error rate (BER) performances of the S/T-equalizers are presented, and performance sensitivity to symbol timing offset is investigated.

key words: *broadband mobile communication, adaptive array antenna, adaptive equalizer, spatial and temporal equalizer, field measurement data*

1. Introduction

The effectiveness of spatial and temporal equalization (S/T-Equalization) in real mobile radio propagation environments has been reported by this letter's companion article [1]. The methodological basis of Ref. [1] is link-level simulations using a two-dimensional (spatial and temporal) channel sounding technique. Channel impulse response data gathered through field measurements were used in the link-level simulations to estimate the real-world performance of S/T-Equalizers. Results of link-level simulations for several S/T-equalizers are presented in Refs. [2]–[4].

The core issue of this letter supplements what is discussed in Ref. [1]. The type of S/T-equalizer investigated in this letter is an L-element adaptive array antenna followed by a maximum likelihood sequence estimator (MLSE). Each of the L antenna elements is equipped with a fractionally spaced tapped delay line (FTDL). For the ease of notation, this S/T-Equalizer configuration is referred to as L-FTDL/MLSE hereinafter. This letter's companion article [1] takes into account the effects of co-channel interference (CCI) on the performance of the same type of S/T-Equalizer.

Manuscript received September 26, 2000.
Manuscript revised February 7, 2001.

[†]The authors are with Wireless Laboratories, NTT DoCoMo, Inc., Yokosuka-shi, 239-8536 Japan.
[††]The author is with Institute for Microelectronics and Mechatronics Systems (IMMS), Langewiesener Str. 22, 98693 Ilmenau, Germany.

Link-level simulation is one type of off-line simulation, but it makes it possible to compare performance on a fair and practical basis since it uses the same field measurement data for different equalization schemes and algorithms. This letter first evaluates the performance of the FTDL/MLSE S/T-Equalizer through link-level simulations using field measurement data gathered in an urban area of Tokyo. The simulations were also conducted using the same data for two other types of S/T-Equalizer: one is an L-element FDTL adaptive array antenna followed by a DFE; the other is an L-element FDTL adaptive array antenna alone (the former is referred to as L-FTDL/DFE, and the latter L-FTDL).

Another discussion topic of this letter is the sensitivity of performance to timing offset from its optimal position. It is shown that for the L-FTDL/MLSE S/T-Equalizer, the sensitivity can be significantly relaxed if the FTDL has sufficient length. This letter is organized as follows: Section 2 shows field measurement data representing the temporal and spatial characteristics of the channel. Section 3 describes the configuration of the S/T-equalizers investigated in this letter. Section 4 shows results of the link-level simulations using the field measurement data.

2. Field Measurements

The two-dimensional channel sounder system [4] was used in the field measurements. Table 1 summarizes major specifications of the field measurement. The channel sounder system makes it possible to identify channel impulse response with sufficient accuracy to permit broadband signal transmission offline simula-

Table 1 Major specifications of field measurement and link-level simulations.

Bandwidth	100 MHz
Radio Frequency	5.2 GHz
Transmitter	Omnidirectional
Reciever	8-element ULA
Tx/Rx Synchronization	Rubidium Reference
Time-domain Resolution	6 nanosec.
Spatial-domain Resolution	2.5 deg.

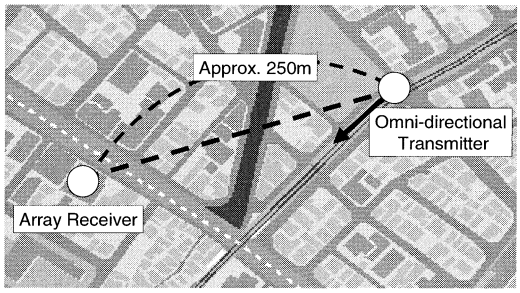

Fig. 1 Measurement environment.

tions. The output of the field measurements is a set of data indicating the impulse responses of the radio channels established between the transmitter's omnidirectional antenna and each of the L elements of the receiver antenna array. The test signal transmitted from the transmitter has a chirp waveform with 100-MHz bandwidth. The carrier frequency is 5.2 GHz. The channel sounder employs FFT-based correlation processing at the receiver. A software utility of the channel sounder system was used to provide a two-dimensional (temporal and spatial) super-resolution signal analysis; its time-domain was 6 *nano*seconds and its spatial-domain resolution was 2.5 degrees.

A series of field measurements took place in a typical urban area of Tokyo prior to the link-level simulations. As shown in Fig. 1, the transmitter was set approximately 250 m from the receiver. Figures 2(A) and (B) show examples of the measurement results: Fig. 2 (A) shows an example of channel impulse response data gathered over 8 seconds of a measurement run; Fig. 2 (B) shows an example of the two-dimensional profile of the received composite signal obtained as a result of the two-dimensional signal analysis. Channel impulse responses last for about 3 *micro*seconds, and the signal components are received over a 90 degree range in azimuth.

3. S/T-Equalizer Configuration

Figure 3 shows a block diagram of the S/T-equalizers evaluated in this letter. Key parameters with the configurations in Fig. 3 are the numbers of the antenna elements (L) and the FTDL taps (M), which are expressed as (L, M) for notation convenience. Another important parameter is the number N of the feedback taps in MLSE. Figure 4(A) shows a block diagram of the MLSE equalizer, where the N feedback taps are used to generate the replicated signal at the array output corresponding to the symbol sequence considered most likely to have been transmitted. The number of the states used by the Viterbi algorithm for MLSE is $Q^{(N-1)}$ for Q-level signaling. For quaternary phase shifted keying (QPSK), $Q = 4$. With L-FTDL/DFE and L-FTDL, the definitions of L, and M are the same as with L-FTDL/MLSE. Figure 4(B) shows a block diagram of the DFE equalizer.

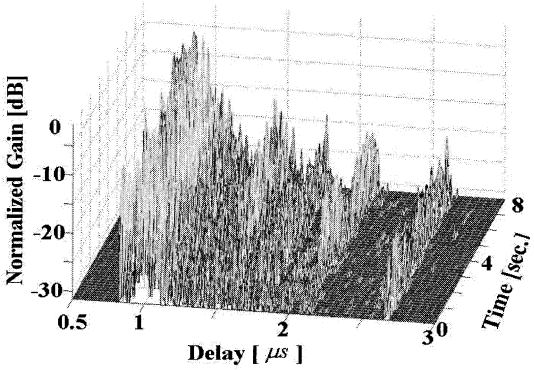

(A) Channel impulse response

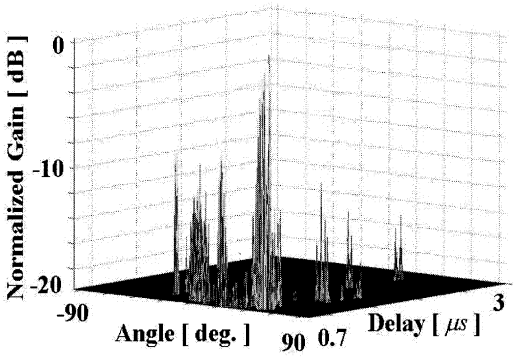

(B) Delay-angular profile

Fig. 2 Example of field measurement data.

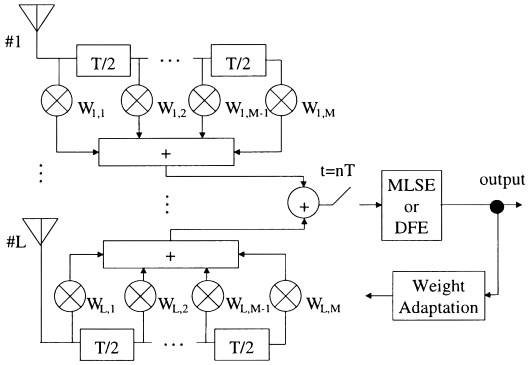

Fig. 3 Block diagram of S/T-equalizer.

Table 2 summarizes major specifications of the signal format used in the link-level simulations. QPSK was used as the modulation scheme. The symbol rate was set at 12 Msymbols/second, which should well support initial studies on future broadband mobile communication systems. The transfer function of a Nyquist filter with roll-off factor $\alpha = 0.5$ was shared equally by the transmitter and receiver. A 12 Mbps QPSK signal was root roll-off filtered at both the transmitter and receiver for spectrum shaping and noise reduction, respectively. All $LM + N$ weights are updated by us-

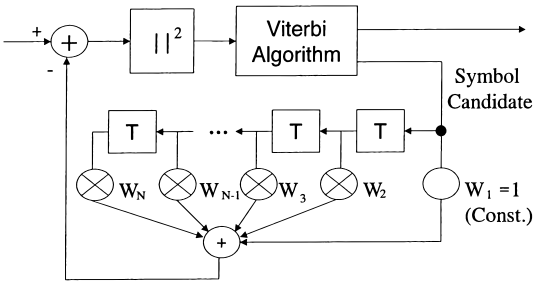

(A) Block diagram of MLSE

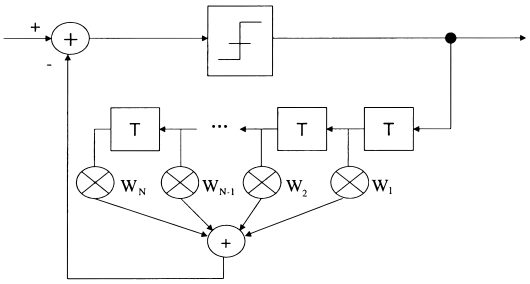

(B) Block diagram of DFE

Fig. 4 Block diagram of temporal equalizer.

Table 2 Major specifications of signal format.

Modulation	QPSK
Symbol Rate	12 Msym./sec.
Tx/Rx Filter	Roor Roll-off, $\alpha = 0.5$
Frame Format	Training: 450 Symbols Data Block: 4960 Guard Block: 40
Adaptive Array	L-element ULA M-tap $T/2$ spaced FFF
Adaptive Equalizer	16-state MLSE, 2-tap DFE
Update Algorithm	RLS, $\lambda = 0.97$

ing the recursive least squares (RLS) algorithm in each symbol timing using the training sequence embedded periodically in the transmitted data frames.

Signal processing in link-level simulations, conducted on a PC platform, included calculating the waveforms of root rolloff-filtered symbol sequences to be transmitted, convolving the transmitted waveforms with the channel impulse response data, and further convolving the channel output with the root rolloff filter's impulse response to obtain the output of the antenna elements. At the receiver, symbol timing was extracted from the desired signal's delay profile. In fact, optimal symbol timing should achieve the best signal transmission performance, but to the author's knowledge, no algorithms for optimal timing extraction that also offer reasonable complexity are known. In this letter, received symbol timing is defined as a timing at which the channel impulse response exhibits its maximum magnitude.

For averaged performance evaluations, the simulation results obtained by using channel impulse response

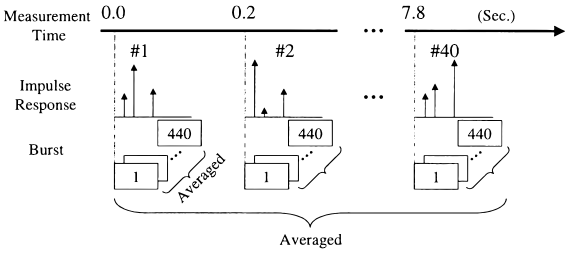

Fig. 5 Operation flow of simulation.

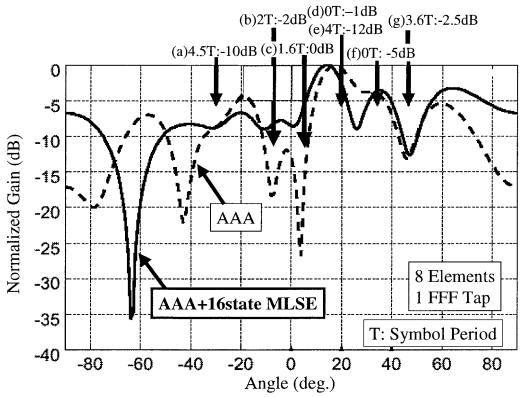

Fig. 6 Beam patterns with L-FTDL and L-FTDL/MLSE. ($L = 8$ and $M = 1$)

data collected in the vicinity of the measurement location of interest have to be averaged. As shown in Fig. 5, channel impulse response data was collected every 1 meter in succession over 8 seconds of the test run for this purpose, resulting in 40 sets of data. In the link-level simulations, 440 bursts were transmitted for each of the 40 sets of the impulse response data, and the performance results for the 17600 ($= 440 \times 40$) bursts were averaged. Assuming very slow fading compared to the burst duration (454 microseconds = 0.2 seconds/440 bursts), impulse response was fixed during each burst.

4. Results

4.1 Performance Comparison

Off-line simulations were conducted using the Tokyo measurement data. Figure 6 shows beam patterns obtained by the link-level simulation. DOAs of major incident signals are indicated in the figure by arrows that lie on their corresponding angles, where their delays and strengths are also described. Such information was obtained as a result of a two-dimensional signal analysis conducted prior to the link-level simulation. The solid and dashed lines indicate the beam patterns formed by L-FTDL/MLSE with $(L, M) = (8, 1)$ and $N = 3$, and L-FTDL with $(L, M) = (8, 1)$, respectively. Both L-FTDL/MLSE and L-FTDL form their patterns so that the signal components indicated by (d) and (f), which have no delay and are relatively strong,

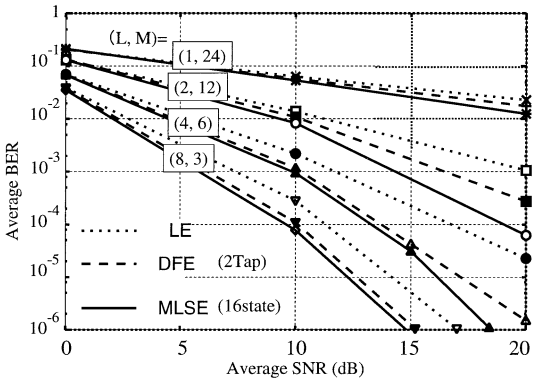

Fig. 7 L-FTDL/MLSE vs. received signal to noise power raio in dynamic condition.

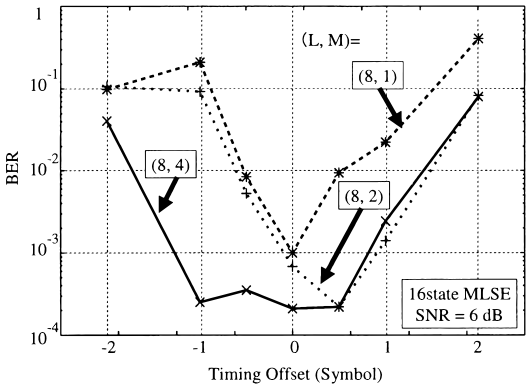

Fig. 8 BER vs. timing offset in static condition.

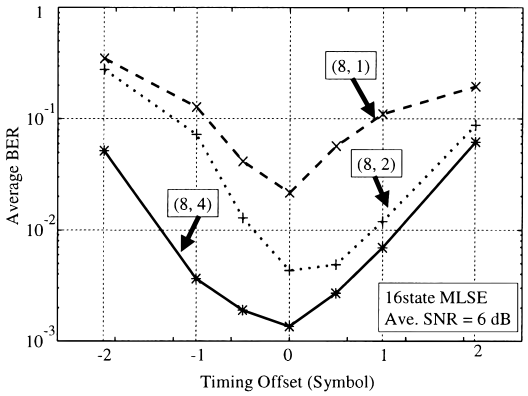

Fig. 9 Average BER vs. timing offset in dynamic condition.

are extracted from the received composite signal. With L-FTDL, the signal components indicated by (b) and (c), which are relatively short-delayed but strong, are nullified, while with L-FTDL/MLSE components (b) and (c) are not nullified. This is because the delays of these components lie within the coverage of the $N = 3$ MLSE equalizer, and hence they are combined. Signal component (g) has $3.6T$ delay (with T being symbol duration), which lies outside MLSE coverage. Hence, with both L-FTDL/MLSE and L-FTDL, it is nullified. Other small signal components having relatively large delays are to be ignored when forming the beam patterns, however, this paper address the detailed behaviors of the algorithms for them.

For a fair comparison of the performance of the three types of S/T-Equalizers, the $L \times M$ value was kept constant at 24. For L-FTDL/MLSE $N \equiv 3$, L-FTDL/DFE $N \equiv 2$, and for L-FTDL $N \equiv 0$. Figure 7 shows average bit error rate (BER) performances for various values of (L, M). It is found that smaller BERs can be achieved with larger L values (hence smaller M values). This indicates that the dominant factor in determining the BER performance is the element numbers of the spatial equalizer. It is found also from Fig. 7 that the use of feedback taps can improve BERs, but the performance difference between L-FTDL/MLSE and L-FTDL/DFE is quite small when $L \geq 4$. In fact, the level of significance should depend on how suitable the channel impulse response is to the S/T-equalizer configuration considered, and hence more significant performance improvement should be achieved by L-FTDL/MLSE under different two-dimensional channel environments.

4.2 Performance Sensitivity to Timing Offset

In practical systems, symbol timing has to be recovered at the receiver, but the optimal timing position cannot always be tracked for all shapes of the channel delay profile. In fact, it is well known that MLSE equalizer performance is sensitive to timing offset [6]. To evaluate the sensitivity of L-FTDL/MLSE's performance to timing offset, 8 times over-sampling with respect to symbol rate T was performed in the link-level simulations. Figure 8 shows for $L = 8$ results of the link-level simulations in a static condition; measurements were made while the transmitter position was fixed. BERs were then evaluated for different timing offset indices with FTDL length M as a parameter. The zero offset in Fig. 8 is the timing at which the channel impulse response exhibits its maximum magnitude. It is found that the BER is quite sensitive to timing offset when $M = 1$ and 2. However, the performance sensitivity is significantly relaxed when $M = 4$. Figure 9 shows results of simulations in a dynamic condition; measurement data were gathered while the transmitter was moving. Hence, the BER curves shown in Fig. 9 indicate average performances, averaged over the data gathered during the measurement run. Even in the dynamic condition, increasing the FTDL length M is effective in reducing the performance sensitivity to timing offset.

5. Conclusions

This letter has shown the results of a series of link level simulations conducted to evaluate the performances

of FTDL/MLSE, L-FTDL/DFE, and L-FTDL S/T-equalizers. Field measurement data gathered in an urban area of Tokyo were used in the link-level simulations. It has been shown that the use of feedback taps can improve BER performance over L-FTDL, but the performance difference between L-FTDL/MLSE and L-FTDL/DFE is quite small when more than 2 feedback taps are used. However, the level of significance should depend on how suitable the channel impulse response is to the S/T-equalizer configuration considered, and hence more significant performance improvement should be achieved by L-FTDL/MLSE under other two-dimensional channel environments. Issues of channel classification in terms of the effectiveness of the S/T-equalizer configurations are left as a future study. Another point this paper has discussed is the performance sensitivity of the L-FTDL/MLSE S/T-equalizer to timing offset. It was shown that increasing the FTDL length is effective in reducing this sensitivity. More data covering various areas will be analyzed in the same way, and results will be presented at a later time.

Acknowledgement

The authors wish to thank Mr. Kazuaki Murota, senior vice president of NTT DoCoMo, Inc. for his encouragement during this research. The authors also wish to thank Mr. Yasuhiro Oda of NTT DoCoMo, Inc. for his support in conducting field measurement data.

References

[1] T. Yamada, S. Tomisato, T. Matsumoto, and U. Trautwein, "Performance evaluation of FTDL-spatial/MLSE-temporal equalizers in the presence of co-channel interference—Link-level simulation results using field measurement data," IEICE Trans. Commun., vol.E84-B, no.7, pp.1961–1964, July 2001.

[2] U. Trautwein, K. Blau, D. Brueckner, F. Hermann, A. Richter, G. Sommerkorn, and R. Thomae, "Radio channel measurement for realistic simulation of adaptive antenna arrays," Proc. 2nd European Personal Mobile Communications Conference, pp.491–498, Sept. 1997.

[3] U. Trautwein, G. Sommerkorn, and R. Thomae, "A simulation study on space-time equalization for mobile broadband communications in an industrial indoor environment," Proc. VTC99, pp.511–515, Houston, May 1999.

[4] U. Trautwein, D. Hampicke, G. Sommerkorn, and R. Thomae, "Performance of space-time processing for ISI- and CCI-suppression in industrial scenarios," Proc. IEEE VTC2000-Spring, pp.1894–1898, Tokyo, May 2000.

[5] K. Fukawa and T. Matsumoto, "A new joint array signal processing structure and maximum likelihood sequence estimation in mobile radio communications," Proc. 4th Workshop on Smart Antennas in Wireless Mobile Communications, Stanford, July 1997.